A Nonlinear Particle Dynamics Map of Wakefield Acceleration in a Linear Collider

T. Tajima, S. Cheshkov, W. Horton and K. Yokoya*

Department of Physics and Institute for Fusion Studies
The University of Texas at Austin
Austin, Texas 78712 USA
* *KEK National Laboratory for High Energy Physics, Japan*

Abstract. The performance of a wakefield accelerator in a high energy collider application is analyzed. In order to carry out this task, it is necessary to construct a strawman design system (no matter how preliminary) and build a code of the systems approach (a typical systems code approach was used, for instance, in SSC studies [1]). A nonlinear dynamics map built on a simple theoretical model of the wakefield generated by the laser pulse (or whatever other method) is obtained and we employ this as a base for building a system with multi-stages (and components) as a high energy collider. The crucial figures of merit for such a system other than the final energy include the emittance (that determines the luminosity). The more complex the system is, the more "opportunities" the system has to degrade the emittance (or entropy of the beam). Thus our map guides us to identify where the crucial elements lie that affect the emittance. We find that a strong focusing force of the wakefield coupled with a possible jitter of the axis (or laser aiming) of each stage and a spread in the betatron frequencies arising from different phase space positions for individual particles leads to a phase space mixing. This sensitively controls the emittance degradation. We show that in the case of a uniform plasma the effect of emittance growth is large and may cause serious problems. We discuss possibilities to avoid it and control the situation.

INTRODUCTION

The use of strong plasma waves excited by laser beams for electron acceleration has been considered [2]. Since then the subject has grown tremendously and become an area of intense research. Many variant acceleration schemes have been suggested: plasma beat wave accelerator, laser wakefield accelerator, plasma wakefield accelerator. These differ in details and how one excites the wakefield or accelerating structure, but the basic idea is common. They also share common mathematical treatment when considered as an element of a system of a large scale accelerator. There are many possible applications of plasma based accelerators and

one of them, perhaps the most challenging, is for construction of a linear collider. It is believed that conventional linear colliders can go up to 1 TeV center of mass energy of colliding particles [3]. However, beyond that probably some new technology needs to enter. A feature of plasma based accelerators is their ability to sustain extremely large acceleration gradients ($\sim 100\,\mathrm{GV/m}$). Correspondingly we can hope to achieve high energy gains on short distance. Such a machine, no doubt, consists of a large number of elements to reach for a desired energy and forms a complex system. In order to identify the most crucial research questions in such a complex problem, it is necessary to design a strawman's system, no matter how simplistic it may be, and to try to analyze and deduce the fundamental properties of such a system. Such a strawman's design was in fact carried out for the first time for a wakefield acceleration-based collider in the last AAC meeting [4]. For an accelerator for high energy physics the energy is one of the important parameters, but there are many others that are crucial for such an accelerator. For instance, low emittance is also necessary. This is because the cross-section of collisions decreases inversely proportional to the energy of the beams and thus we need high luminosity to detect new physics. The requirement for luminosity, in turn, demands for low emittance. The geometrical luminosity is given by

$$\mathcal{L} = \frac{f_c N^2}{4\pi\sigma_x\sigma_y}, \tag{1}$$

where f_c is the collision frequency, N is the particle number per bunch and σ_x and σ_y are the r.m.s. beam sizes at the IP (interaction point). Thus, it is important to analyze the performance of laser wakefield accelerators not only energy-wise but also with respect to all other relevant beam parameters. The first thing to notice is that the whole acceleration process takes place over a period too short for ions to move. Therefore the analysis may be limited to considering the electron motion only in a background of immobile ions. This not only simplifies analysis, but (generally speaking) stabilizes the system, as immobile ions anchor electrons and photons. In most scenarios the desired final energy of accelerating particles ($\sim$ TeV) cannot be achieved over a single acceleration stage. Thus we need to evaluate the effects associated with multistaging and to analyze the complete acceleration process. In the present investigation we limit ourselves to the linear regime of wakefield generation. A major simplification arises from the separate treatment of beam electrons and plasma electrons. The plasma electrons are supporting the wakefield but not trapped by it. This is the sequence of the linear regime. On the other hand, the beam electrons are affected (accelerated and focused) by the wakefield.

In Sec.2 of this paper we analyze the Laser Wakefield Accelerator (LWFA) in the case of an initially homogeneous plasma and obtain expressions in a similar way as in [5] for the longitudinal and radial wakefields in the case of cylindrical geometry. The motion of an accelerated particle beam is considered in Sec.3. With the help of some simplifying assumptions valid in the ultrarelativistic case, we integrate the single particle motion. Based on the single stage analytical results, in Sec.4 we derive a map for multistage LWFA, which is used as a base for a tracking code.

Considering the target center of mass energy $E_{cm} = 5$ TeV and luminosity $\mathcal{L}_g = 10^{35}$ cm^{-2}s^{-1} in [4], it is shown that for a fixed power P_b of the colliding beams there are only two independent parameters describing the beam at IP: the number of particles per bunch N and the longitudinal beam size σ_z (we assume a round beam: the aspect ratio $R = 1$). All other beam parameters at IP can be expressed as functions of the above. So we know what the requirements on the normalized emittance are.

In Sec.5 we analyze the effect of random dislocations of the accelerating stages on the beam emittance. These dislocations combined with unavoidable spread in individual particle betatron frequencies lead to a considerable emittance growth which may require alternative LWFA design. Conclusions are drawn in Sec.6.

WAKEFIELD MODEL

A short high power laser pulse propagating in plasma can excite wakefields which may be used for acceleration of charged particles. In the linear regime the plasma responds to the ponderomotive force acting on plasma electrons:

$$\mathbf{F} = e\nabla\Phi_l(r,z,t)\,, \tag{2}$$

where the ponderomotive potential Φ_l is connected with the laser vector potential A_l:

$$\Phi_l(r,z,t) = -\frac{m_e c^2}{2e} a_0^2(r,z,t)\,,$$

$$a_0 = \frac{eA_l}{m_e c^2}\,, \tag{3}$$

and a_0 is the normalized vector potential. The plasma response to this force can be obtained from the cold fluid equations ([5]):

$$\tfrac{d}{dt}\mathbf{v} = -\tfrac{e}{m_e\gamma}\left\{\mathbf{E} + \tfrac{1}{c}\mathbf{v}\times\mathbf{B} - \tfrac{1}{c^2}\mathbf{v}(\mathbf{v}\cdot\mathbf{E})\right\}, \tag{4}$$

$$\tfrac{\partial}{\partial t} n + \nabla\cdot n\mathbf{v} = 0, \tag{5}$$

where n is the electron density and γ is the Lorenz factor. These equations could be solved perturbatively, assuming that the density perturbation is relatively small.

For a laser pulse of the form (with a pulse length l_l, spot radius r_s)

$$\mathbf{A_l} = \begin{cases} \mathbf{A_{l0}} \sin\left(\frac{\pi\xi}{l_l}\right) \exp\left(-\frac{r^2}{r_s^2}\right), & 0 < \xi < l_l\,, \\ 0, & \text{otherwise}\,, \end{cases} \tag{6}$$

where $\xi = z - ct$, the maximum electric field in the z-direction behind the pulse ($\xi < 0$) is

$$E_z(\xi, r) = \frac{\pi^2}{l_l}\,\Phi_{l0}\exp\left(-\frac{2r^2}{r_s^2}\right)\cos\left(2\pi\xi/l_l\right), \tag{7}$$

where Φ_{l0} is given by

$$\Phi_{l0} = -\frac{m_e c^2}{2e}a_0^2\,. \tag{8}$$

The maximum field (7) is reached when the resonance condition is satisfied: $\lambda_p \approx l_l$, where λ_p is the plasma wave wavelength $2\pi c/\omega_p$. The transverse electric field E_r and magnetic field B_θ are generated according to the Panofski–Wenzel theorem [6]

$$\frac{\partial E_z}{\partial r} = \frac{\partial(E_r - B_\theta)}{\partial \xi}, \tag{9}$$

leading to

$$(E_r - B_\theta) = -\frac{2\pi}{r_s^2}\Phi_{l0} r \exp\left(-\frac{2r^2}{r_s^2}\right)\sin\left(2\pi\xi/l_l\right). \tag{10}$$

We observe that for a relativistic particle ($v_z \approx c$) the transverse force will be proportional to $(E_r - B_\theta)$. There is a region in the wake (quarter period) where a relativistic electron experiences simultaneous acceleration and transverse and longitudinal focusing. This feature of the LWFA makes it different from the conventional accelerators and we do not need the alternating gradient principle here. At the same time, however, it may pose a problem, as we shall see in Sec.5. The wakefield structure of this model is common to other sisters of wakefield accelerators such as PBWA and PWA (See, for example, [7]).

ELECTRON MOTION IN THE PLASMA WAKEFIELD

The main acceleration follows an electron injector which can be used as a charged particle source for our accelerator. Designing such an injector is a task itself (e.g. [8], [9], [10]), but we leave it to investigation elsewhere.

We consider the motion of high energy electrons of the beam in the plasma wakefield. The complicated problem may be simplified to obtain the essential dynamics as far as the beam particle dynamics is concerned with the following assumptions:

1. The region in the phase space occupied by the beam is small.

2. The wakefield is not affected by the beam (the beam loading effect, however, will be considered in a follow up paper to be published in the same proceedings).

3. The particles in the beam are highly relativistic and move predominantly in z-direction (which is the direction of propagation of the laser pulse).

$$\dot{z} \gg \dot{x}, \dot{y}$$

$$\dot{z} \approx c$$

4. The motions in x and y are decoupled.

5. No interaction among the beam particles.

6. The laser pulse does not evolve.

These assumptions do not take into account a significant part of the physics of all the processes. Work in progress on the problem will relax some of these assumptions. The wakefield generated by the beam can be included in the considerations using the results in [11]. This will be carried out in a follow-up paper to be published in the present proceedings. Assumption 5 is probably good enough for high energy particles and relatively low currents, because the space charge force diminishes by a factor of $1/\gamma^2$. Assumption 6 is related to the pump-depletion problem [12] and also should be taken into account in the future.

Starting with the single particle equation of motion

$$\frac{d\mathbf{p}}{dt} = -e\left(\mathbf{E} + \frac{\mathbf{v}\times\mathbf{B}}{\mathbf{c}}\right), \tag{11}$$

and assuming that the beam particles are close to the z-axis, we obtain the following basic system of differential equations for the longitudinal motion

$$\frac{d\gamma}{d\hat{z}} = \Phi_0 \cos\Psi, \tag{12}$$

$$\frac{d\Psi}{d\hat{z}} = 1 - \frac{\beta_p}{\beta}, \tag{13}$$

where Ψ is the particle phase with respect to the wakefield. For the transverse motion

$$\frac{d\hat{p}_u}{d\hat{z}} = -\frac{4\Phi_0}{r_s^2}\hat{u}\sin\Psi, \tag{14}$$

$$\frac{d\hat{u}}{d\hat{z}} = \frac{\hat{p}_u}{\gamma k_p^2}, \tag{15}$$

where

$$\beta_p = \sqrt{1-(v_p/c)^2}, \quad \Phi_0 = \frac{e\pi E_0 a_0^2}{4k_p m_e c^2} = \frac{\pi a_0^2}{4}, \tag{16}$$

$$\hat{z} = k_p z\,, \quad \hat{u} = u\,, \quad \hat{p}_u = \frac{k_p}{m_e c}\, p_u\,. \tag{17}$$

Here $E_0 = cm_0\omega_p/e$, $k_p = \omega_p/c$, v_p is the phase velocity of the wake and u and p_u stand for transverse variables x and p_x or y and p_y. After convenient normalizations, the important points are that we use $k_p\, z$ as our time coordinate and the energy and the phase of the particles with respect to the wake are our 'longitudinal' variables.

Equations (12), (13) decouple from (14) and (15) and we can consider these two sets independently. The first set is conveniently analyzed using the following one-dimensional Hamiltonian [13]:

$$H = \gamma(1 - \beta\beta_p) + \Phi(\Psi), \tag{18}$$

where

$$\Phi(\Psi) = -\Phi_0 \sin\Psi. \tag{19}$$

In the phase space formed by the first pair of variables (γ, Ψ) we have stable fixed points: $\gamma = \gamma_p$ and $\Psi = \pi/2 + 2n\pi$ and unstable fixed points: $\gamma = \gamma_p$ and $\Psi = -\pi/2 + 2n\pi$.

There are two phase space regions – trapped, where the particles execute bounded motion and untrapped one, where the motion is unbounded in Ψ direction [1] (see Figure 1). Because we are primarily interested in high energy physics applications of wakefield accelerator here, we consider the untrapped case, where the particle orbits are well above the separatrix. It is important to understand that even initially we have very high energy particles, so the upper untrapped region is our operating region.

We can further simplify the equations of motion for γ and Ψ by putting $\beta = 1$ to obtain:

$$\frac{d\gamma}{d\hat{z}} = \Phi_0 \cos(\Psi)\,, \tag{20}$$

$$\frac{d\Psi}{d\hat{z}} = \frac{1}{2\gamma_p^2}, \tag{21}$$

where $\gamma_p = 1/\sqrt{1-\beta_p^2}$. These equations are integrated directly to give

$$\Delta\gamma = 2\Phi_0\gamma_p^2(\sin\Psi - \sin\Psi_0)\,, \tag{22}$$

$$\Psi = \Psi_0 + \frac{\hat{z}}{2\gamma_p^2}\,, \tag{23}$$

where $\hat{z} = k_p z$ and Ψ_0 is the initial phase of the particle with respect to the wakefield. First we observe that the maximum energy gain is $2\Phi_0\gamma_p^2$ and taking

---

[1] the graph is not to scale.

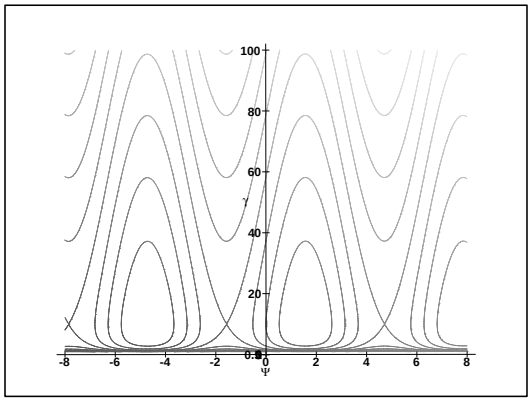

FIGURE 1. The phase space: electron Lorentz factor γ vs. the phase with respect to the wakefield Ψ.

typical values of the parameters $\Phi_0 = 0.2$ (which corresponds to $a_0 = 0.5$ [2]) and $\gamma_p = 100$ we see that the above gain is about $4 \cdot 10^3$ in units of electron's rest energy or in other words about 2 GeV. This energy is achieved over a 'distance' $\hat{z}$ of $3 \cdot 10^4$ which is about 50 cm. The actual gain will be smaller if the pump depletion [12] is taken into account. Keeping in mind this tentative 'design' of one stage, we now look at the multistaging effects.

MULTISTAGE ACCELERATION

When we try to accelerate particles to TeV energies, we need to investigate problems associated with the multistaging. In order to carry this out, we would like to obtain a map which describes the one to one correspondence between the entrance coordinates and the exit coordinates of the beam particles during the propagation of the beam trough many accelerating stages and use it to build a systems code. As in the standard RF linac theory, we have a reference particle moving along the ideal (design or synchronous) orbit. All other particles in the bunch will be described by their relative position with respect to the reference one.

The linearized equations of motion for the longitudinal degrees of freedom are:

$$\delta\Psi_{n+1} = \delta\Psi_n \tag{24}$$

$$\delta\gamma_{n+1} = 2\gamma_p^2\Phi_0(\cos(\Psi_s + \Delta) - \cos(\Psi_s))\delta\Psi_n + \delta\gamma_n, \tag{25}$$

where n enumerates the stage, Ψ_s is the 'synchronous' phase, Δ is the phase slippage per accelerating stage (actually it can also depend on n). Because of the fact that we are considering extremely high energy particles ($\gamma \sim 10^5 - 10^7$) the equation (24) decouples from (25) (There is a very small coupling term $\sim 1/\gamma^2$). Formally

[2] We take $a = 0.5$ to be still in the 'controlled' linear regime.

the equations look the same as in standard linac theory when the synchrotron oscillation frequency approaches zero. However, the physical regime of operation is quite different from the RF linac – we have a significant phase slippage over a stage (it is precisely this slippage which gives us the energy gain). And it also limits the maximum possible gain per stage. This difference comes from the fact that the plasma wave is relatively "slow" ($\gamma_p \approx 100$, instead of ∞). From equations (24) and (25) we see that in the approximation we are working in the phases of the particles do not change and the absolute energy spread increases linearly with the stage number (actually this is the beginning of a very slow synchrotron oscillation which happens on a time scale much greater than the time it takes a particle to travel the whole accelerator).

Now let us consider the transverse motion. It is described by

$$\ddot{\tilde{u}} + \left[\omega_\beta^2 \sin\left(\omega_s \hat{z} + \Psi_s + \delta\Psi_n\right) - \frac{1}{2}\frac{\ddot{\gamma}}{\gamma} + \frac{1}{4}\frac{\dot{\gamma}^2}{\gamma^2}\right] \tilde{u} = 0\,, \tag{26}$$

where

$$\omega_s = \frac{1}{2\gamma_p^2}\,, \tag{27}$$

$$\omega_\beta = \left(\frac{4\Phi_0}{\gamma (k_p r_s)^2}\right)^{1/2}\,, \tag{28}$$

$$\tag{29}$$

and $\tilde{u} = \sqrt{\gamma}\; u$. In the high energy regime the third term in the square brackets in (26) is negligible and the second term is usually also small because of the proportionality to $1/\gamma_p^2$. Still, in the cases of very weak focusing we have to take it into account (for instance, in plasma channel).

More generally, the equation we are considering is Hill's equation:

$$\ddot{\tilde{u}} + f(\hat{z})\tilde{u} = 0. \tag{30}$$

An analytic solution can be found when some additional approximations are used. We treat two simple cases where we can obtain analytical results easily before we discuss the general case. The simplest and the first thing to do is to approximate the focusing function in (30) by some constant value and then the equation describes just a simple harmonic oscillator. We adopt this, and also assume just a free drift (which can be replaced by magnets, if necessary) of the particles between the stages. Let us forget for a moment that the particles are being accelerated, and that the strength of the focusing force actually depends on the stage even if the stages are physically identical. To get a stable solutions we need to satisfy:

$$|\mathrm{Tr}\, M| < 2, \tag{31}$$

where M is the transfer matrix:

$$M = \begin{pmatrix} \cos(\frac{\omega}{\omega_s}\Delta), & \frac{1}{\omega}\sin(\frac{\omega}{\omega_s}\Delta) \\ -\omega\sin(\frac{\omega}{\omega_s}\Delta), & \cos(\frac{\omega}{\omega_s}\Delta) \end{pmatrix} \cdot \begin{pmatrix} 1 & \hat{L} \\ 0 & 1 \end{pmatrix}, \tag{32}$$

where Δ is the phase advance of the particle per stage with respect to the wakefield and $\hat{L}$ is the length of the distance between the stages in units of k_p^{-1}. ($1/\omega$ is betatron length in units k_p^{-1}). The matrix (32) can be written as

$$M = \begin{pmatrix} \cos(\frac{\omega}{\omega_s}\Delta), & \frac{1}{\omega}\sin(\frac{\omega}{\omega_s}\Delta) + \hat{L}\cos(\frac{\omega}{\omega_s}\Delta) \\ -\omega\sin(\frac{\omega}{\omega_s}\Delta), & -\hat{L}\omega\sin(\frac{\omega}{\omega_s}\Delta) + \cos(\frac{\omega}{\omega_s}\Delta) \end{pmatrix}. \tag{33}$$

The map $\mathcal{M}$ for the total accelerator system is

$$\mathcal{M} = M^N, \tag{34}$$

where N is the total number of stages. When we do not have any drift space, the solutions are always stable. If we increase $\hat{L}$ keeping the other parameters fixed at some point we reach a "blow-up" of emittance. So the maximum distance between the stages is limited. The trace of M is:

$$\mathrm{Tr}M = 2\cos\left(\frac{\omega}{\omega_s}\Delta\right) - \omega\hat{L}\sin\left(\frac{\omega}{\omega_s}\Delta\right) \tag{35}$$

and for stability it should satisfy (31). This result was used to check the map code – up to a some value of L there is no emittance growth (see Figure 2) and after that we indeed find the "blow up".

Now, this calculation does not take into account the fact that particles accelerate and ω_β is decreasing ($\omega_\beta = \sqrt{\frac{4\Phi_0}{\gamma(k_p r_s)^2}}$). Also in reality particles have different (random) phases with respect to the wakefield and different energies which causes a spread in the individual particle betatron frequencies. Therefore , the above analysis should be done for each particle separately, but if the differences in their phases are small the conditions for stable motion are practically the same for all the particles.

The other case is when the argument of the sine in (26) is relatively small and we can use $\sin(x) \approx x$. In this case (26) reduces to

$$\ddot{\tilde{u}} - z'\tilde{u} = 0, \tag{36}$$

whose solutions are well known – they are expressible as linear combination of the Airy functions $Ai(z')$ and $Bi(z')$.

In the general case we can do the following analysis. Suppose we know two fundamental solutions to (30) when $\delta\Psi_n = 0$. Say $\tilde{u}^1(\hat{z})$ and $\tilde{u}^2(\hat{z})$. Then

$$\tilde{u} = C_1\tilde{u}^1(\hat{z}) + C_2\tilde{u}^2(\hat{z}). \tag{37}$$

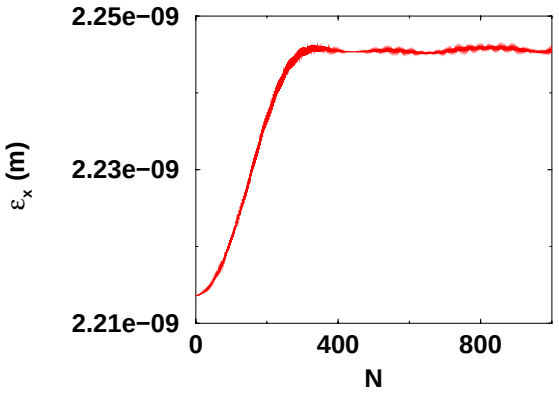

FIGURE 2. The normalized x-emittance ϵ_x vs. stage number N; γ_p=100, $\hat{L}$=10000, ϵ_x^0=2.2 nm, r_s=0.5mm, $a_0 = 0.5$, no acceleration, no dislocations, $\delta\gamma/\gamma$=0.01, $\delta\Psi = 0.01$.

And let us assume that

$$\tilde{u}^1(0) = 1, \qquad \dot{\tilde{u}}^1(0) = 0 \tag{38}$$

$$\tilde{u}^2(0) = 0, \qquad \dot{\tilde{u}}^2(0) = 1\,, \tag{39}$$

so that

$$\tilde{u}_{n+1} = \tilde{u}_n\tilde{u}^1(\hat{l}) + \dot{\tilde{u}}_n\tilde{u}^2(\hat{l}) \tag{40}$$

$$\dot{\tilde{u}}_{n+1} = \tilde{u}_n\dot{\tilde{u}}^1(\hat{l}) + \dot{\tilde{u}}_n\dot{\tilde{u}}^2(\hat{l})\,. \tag{41}$$

For a particle which has some finite $\delta\Psi_n$, equation (30) becomes

$$\ddot{\tilde{u}} + f(\hat{z} + \delta\Psi_n/\omega_s)\tilde{u} = 0, \tag{42}$$

where $f(\hat{z})$ is the same (as a function) as in (30). In this case

$$\tilde{u} = C_1\tilde{u}^1(\hat{z} + \delta\Psi_n/\omega_s) + C_2\tilde{u}^2(\hat{z} + \delta\Psi_n/\omega_s)\,. \tag{43}$$

It can be shown easily that

$$\tilde{u}_{n+1} = \tilde{u}_n\left(\dot{\tilde{u}}^2(\delta\Psi_n/\omega_s)\tilde{u}^1(\hat{l} + \delta\Psi_n/\omega_s) - \dot{\tilde{u}}^1(\delta\Psi_n/\omega_s)\tilde{u}^2(\hat{l} + \delta\Psi_n/\omega_s)\right) +$$

$$+\dot{\tilde{u}}_n\left(\tilde{u}^1(\delta\Psi_n/\omega_s)\tilde{u}^2(\hat{l} + \delta\Psi_n/\omega_s) - \tilde{u}^2(\delta\Psi_n/\omega_s)\tilde{u}^1(\hat{l} + \delta\Psi_n/\omega_s)\right)\,, \tag{44}$$

and

$$\dot{\tilde{u}}_{n+1} = \tilde{u}_n\left(\dot{\tilde{u}}^2(\delta\Psi_n/\omega_s)\dot{\tilde{u}}^1(\hat{l} + \delta\Psi_n/\omega_s) - \dot{\tilde{u}}^1(\delta\Psi_n/\omega_s)\dot{\tilde{u}}^2(\hat{l} + \delta\Psi_n/\omega_s)\right) +$$

$$+\dot{\tilde{u}}_n\left(\tilde{u}^1(\delta\Psi_n/\omega_s)\dot{\tilde{u}}^2(\hat{l} + \delta\Psi_n/\omega_s) - \tilde{u}^2(\delta\Psi_n/\omega_s)\dot{\tilde{u}}^1(\hat{l} + \delta\Psi_n/\omega_s)\right)\,. \tag{45}$$

The point here is that even though in general $\tilde{u}^1(\hat{z})$ and $\tilde{u}^2(\hat{z})$ cannot be found in analytical form and we need to find them numerically it has to be done only once, because they are the same for all the particles. This is an exact statement only if we neglect spread in γ, in general it is not possible, and then the solution is to linearize (30) assuming $\delta\gamma$ and $\delta\Psi$ small and then do perturbation analysis. Of course the above analysis would modify the map but it is not going to change the final results significantly. So, in general (of course, we again incorporate the drift space),

$$\mathcal{M} = M_N M_{N-1} ... M_2 M_1 \,. \tag{46}$$

We note that because of the common structure of the wakefield in all plasma based accelerators the obtained map, with just slight modifications, can be used to analyze their performance as well.

We coded the map in the case of a constant betatron frequency (a different constant for each stage and each particle depending on the stage number and particle distribution in the $(\gamma\,, \Psi)$ phase space) and tests showed that when we start with a normalized r.m.s. emittance of $\epsilon_u = 2.2\,\mathrm{nm}$ (and in the code particles of course get accelerated) up to some value of the drift space the emittance is preserved (See Figure 3). This emittance corresponds to the 5 TeV design I presented in [4].

JITTER AND NOISE

For a complex system cumulative errors can give rise to a surprising (and often unpleasant) result. We identify that one of the most important such effects stems from the transverse jitter of the aligned wakefield (by whatever mechanism) stage by stage. The problem here is that up to this point we have not considered possible dislocation of the consequent stages. This, combined with the fact that the focusing force is different for different particles can lead to a severe emittance growth. Basically, what happens is that all particles rotate at different angular velocities in the phase space and if there is a stage position shift present, we get a characteristic "banana" shaped distribution (it is "banana" shaped only if the dislocation size is larger than the beam size, but in any case the particle distribution gets diluted because of the misalignments). This process critically depends on the magnitude of the betatron frequency spread which means that the typical strength of the focusing force is of great importance. The effect of plasma noise (or other noise, such as laser or the boundary) on the particle dynamics over a stage may be incorporated in a map similar to the stage-by-stage jitter. Such dynamics results in a fuzzy or stochastic [14] map.

We consider the case of stage jitter (in reality there are longitudinal stage jitters as well, but in this paper we restrict ourselves to the transverse case only). The dislocation of the aligned position of each stage is given in our code as a stochastic variable which has a Gaussian distribution. The map is modified according to:

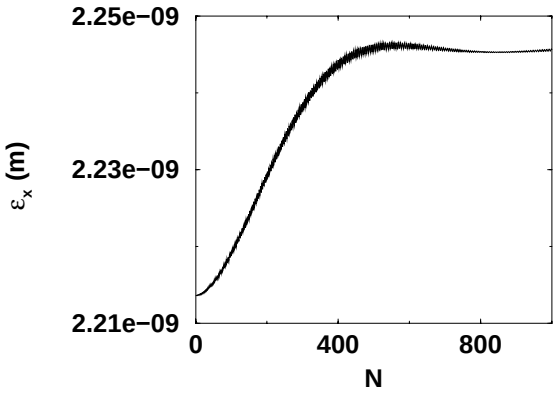

FIGURE 3. The normalized x-emittance ϵ_x vs. stage number N; γ_p=100, $\hat{L}$=10000, ϵ_x^0=2.2 nm, r_s=0.5mm, $a_0 = 0.5$, no dislocations, $\delta\gamma/\gamma$=0.01, $\delta\Psi = 0.01$.

$$\begin{pmatrix} \tilde{x}_{n+1} \\ \dot{\tilde{x}}_{n+1} \end{pmatrix} = M_n \begin{pmatrix} \tilde{x}_n - \tilde{\mathcal{D}} \\ \dot{\tilde{x}}_n \end{pmatrix} + \begin{pmatrix} \tilde{\mathcal{D}} \\ 0 \end{pmatrix} , \tag{47}$$

where $\mathcal{D}$ is the misalignment size ($\tilde{\mathcal{D}} = \sqrt{\gamma_n}\mathcal{D}$). The longitudinal degrees of freedom are not affected. Run with random dislocations of magnitude $\sigma_{\mathcal{D}} = 1 \cdot 10^{-7}$ m is presented in Figure 4 and Figure 5. We see that in this case (corresponds to design I [4]) we have a severe emittance growth (the initial normalized emittance is 2.2 nm). We have to point out that even though there are cases corresponding to large spot sizes which preserve the normalized emittance quite well their practical realization would require a huge laser power probably well above any future experimental limits. The other possible way to cure the situation is to increase the number of stages (and decrease γ_p) which also does not seem plausible (it may be difficult practically to have more than a thousand stages). To control the laser aiming and beam position better than 0.1 μm during the acceleration process is also not promising. In general, the way to alleviate the situation is to decrease the strength of the focusing force. Here comes the idea of possible use of a preformed hollow plasma channel [15]. The conclusion is that the problem is quite serious and should be analyzed in detail. We do this in a follow up paper to appear in the same proceedings. Here we just note that in the case of a initially uniform plasma, for typical values of parameters, we encounter a severe emittance growth in the presence of small stage jitters. The difficulty is primarily due to the fact that the wakefield focusing force is too large in this case. We should also remember that the above considerations do not include any nonlinear effects which also contribute to the phase area increase, not to mention that in addition to all of the above we have to come up with a mechanism for guiding of the laser pulse (when the laser spotsize is small), otherwise the diffraction may limit significantly the acceleration length which is incompatible with our design.

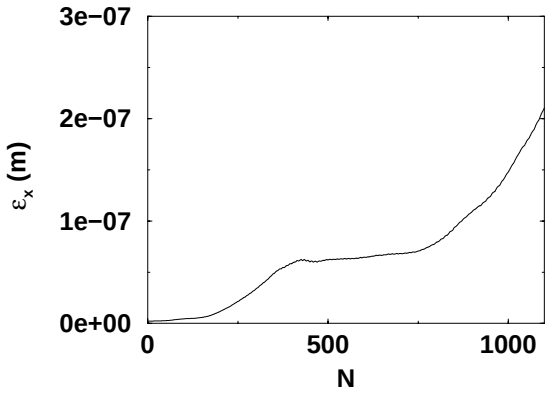

FIGURE 4. The normalized x-emittance ϵ_x vs. stage number N; γ_p=100, laser wavelength $\lambda = 1\mu$m, $\hat{L}$=10000, ϵ_x^0=2.2 nm, r_s=0.5mm, $a_0 = 0.5$, dislocation size = 0.1μm, $\delta\gamma/\gamma$=0.01, $\delta\Psi = 0.01$. The final energy is 2.5 TeV.

CONCLUSION

We studied the cumulative effects of the successive acceleration, transport, and focusing in the laser wakefield (or its sister methods) over many stages. Such cumulative dynamical behaviors are important to investigate for real world accelerators such as a high energy collider. Errors arising from the jitter of each stage or equivalently (in our map approach) the noise in the system can accumulate in such a way to degrade some of the parameters of the beam. The most crucial of these may be the emittance (or the entropy) of the beam. We showed that a set of stages with an ideal wakefield acceleration, drift, and focusing can preserve even a very small emittance over a thousand stages while the energy of the accelerated particles reaches the goal of 5 TeV center of mass energy.

When we have stochastic variables on the wakefield (we chose the stage jitter of the axis of the wakefield in particular), the emittance can significantly increase over the many stages due to the strong focusing of the wakefield. This is probably the most serious effect on the long range behavior of the beams in this kind of accelerator for high energy applications. Search for the best parameter set in the multidimensional parameter space of a large scale accelerator should be performed taking into account, to our best notion, future experimental limits and restrictions which might come from them. The last point we would like to make is that the proposed map for LWFA gives us an opportunity to study not only effects of stage jitter, but also effects which come from other random sources i.e. plasma noise. The noise enter our map equations in the form of random kicks in the r.h.s. of (24) and (25). To be able to do this, we need the statistical distributions of these kicks, which will be presented in a future publication. The work is supported by US DoE.

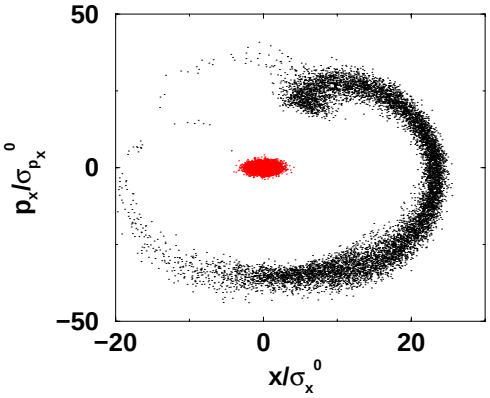

FIGURE 5. The phase space p_x vs. x. corresponding to Figure 4. The original distribution is taken Gaussian (beam is assumed initially matched, so $\sigma_x^0 = \sqrt{\epsilon_x^0 \beta_x^0/\gamma^0}$ and $\sigma_{p_x}^0 = \sigma_x^0/\beta_x^0$) and the final after 1100 acceleration stages.

REFERENCES

1. Yan, Y., Naples, J. and Syphers, M., eds., *Accelerator Physics at the SSC* (AIP, New York 1995).
2. Tajima, T. and Dawson, J., *Phys. Rev. Lett.* **43**, 267-270 (1979).
3. The NLC Design Group and NLC Physics Working Group. *Physics and technology of the Next Linear Collider.* A Report Submitted to Snowmass 96 (1996).
4. Xie, M., Tajima, T., Yokoya, K. and Chattopadhyay, S., "Studies of laser-driven 5 TeV e^+e^- colliders in strong quantum beamstrahlung regime", *Advanced Accelerator Concepts 7* (AIP, New York 1997conf), p.233-242.
5. Esarey, E., Ting, A., Sprangle, P. and Joyce, G., *Comments Plasma Phys. Controlled Fusion* **12**, 191–204 (1989).
6. Chen, P., *Part. Accelerators* **20**, 171–182 (1985).
7. Breizman, B., Fisher, D., Chebotaev, P. and Tajima, T., *IFS report, University of Texas at Austin* **502**, (1991).
8. Rau, B., Tajima, T. and Hojo, H., *Phys. Rev. Lett.* **78**, No. 17, 3310–3313 (1997).
9. Umstadter, D., Kim, J. and Dodd, D., *Phys. Rev. Lett.* **76**, No. 12, 2073–2076 (1996).
10. Esarey, E., Hubbard, R., Leemans, W., Ting, A. and Sprangle, P., *Phys. Rev. Lett.* **79**, No. 14, 2682–2685 (1997).
11. Katsouleas, T., Wilks, S., Chen, P., Dawson, J. and Su, J., *Part. Accelerators* **22**, 81–98 (1987).
12. Horton, W. and Tajima, T. *Phys. Rev. A* **34**, 4110–4119 (1986).
13. Esarey, E., Sprangle, P., Krall, J. and Ting, A., *IEEE Trans. Plasma Science* **24**, No. 2, 252–288 (1996).
14. Van Kampen, N., *Phys. reports* **24**, No. 3, 171–228 (1976).
15. Chiou, T., Katsouleas, T., Decker C., Mori, W., Wurtele, J., Shvets, G. and Su., J., *Phys. Plasmas* **2**, No. 1, 310–318 (1995).